

**Lattice Boltzmann method for Lennard-Jones fluids based on the gradient theory of interfaces**

E. S. Kikkinides

*Department of Mechanical Engineering, University of Western Macedonia, 50100 Kozani, Greece*

M. E. Kainourgiakis, A. G. Yiotis, and A. K. Stubos

*Environmental Research Laboratory, National Center for Scientific Research "Demokritos", 15310 Ag. Paraskevi, Athens, Greece*

(Received 12 July 2010; revised manuscript received 16 September 2010; published 8 November 2010)

In the present study we propose a lattice Boltzmann equation (LBE) model derived from density gradient expansions of the discrete BBGKY evolution equations. The model is based on the mechanical approach of the gradient theory of interfaces. The basic input is the radial distribution function, which is related exclusively to the molecular interaction potential, rather than semiempirical equations of state used in previous LBE models. This function can be provided from independent molecular simulations or from approximate theories. Evidently the accuracy of the interaction potential, and thus the radial distribution function, reflects on the accuracy of the thermodynamic properties and consistency of the derived LBE model. We have applied the proposed model to obtain equilibrium bulk and interfacial properties of a Lennard-Jones fluid at different temperatures,  $T$ , close to critical,  $T_c$ . The results demonstrate that the LBE model is in excellent agreement with gradient theory as well as with independent literature results based on different molecular simulation approaches. Hence the proposed LBE model can recover accurately bulk and interfacial thermodynamics for a Lennard Jones fluid at  $T/T_c > 0.9$ .

DOI: [10.1103/PhysRevE.82.056705](https://doi.org/10.1103/PhysRevE.82.056705)

PACS number(s): 47.11.-j, 02.70.Ns, 05.70.Np, 68.03.Cd

**I. INTRODUCTION**

Interfacial phenomena and liquid-vapor phase transitions have an important impact in many natural and commercial processes of industrial or environmental importance. Consequently, the proper description of the structure of the liquid-vapor interface and the corresponding surface tension require a detailed molecular theory for the statistical mechanics of nonuniform fluids [1]. The modern theory of interfaces has its origins in the seminal works of Rayleigh, van der Waals and their successors [2]. Based on van der Waal's theory, later revived by Cahn and Hilliard [3], a thermodynamic gradient theory of interfaces has been developed to describe the behavior of inhomogeneous fluids by seeking a Helmholtz free energy as a functional of fluid density distributions, which can be determined by minimizing this energy at isothermal conditions. Minimization of Helmholtz free energy generates functional expressions for the chemical potentials, which must be constant at equilibrium, resulting in differential or integral equations for the fluid density [3–6]. In an alternative way, known as the mechanical approach of gradient theory, one starts from momentum or force balances, the well known Bogoliubov-Born-Green-Kirkwood-Yvon (BBGKY) equations, where only mechanical equilibrium is guaranteed. The pressure tensors that appear in these equations are functionals of the density distribution. Taking density gradient expansions of the BBGKY equations we obtain, at steady state, hydrostatic differential equations for the fluid density that are of different order compared to those of the thermodynamic approach [6,7]. At some special cases the mechanical approach can also preserve chemical equilibrium and it has been shown that in this case the two theories produce almost identical results in terms of density distributions and interfacial properties [6–8]. The main limitation of gradient theory is the assumption of slowly varying density across an interface, which mathematically holds only at tem-

peratures,  $T$ , that are very close to the critical temperature,  $T_c$ . Nevertheless, practice has revealed that this assumption is still valid at temperatures that can be as low as 90% of the critical temperature (i.e.,  $T/T_c > 0.9$ ) [2]. Another limitation of the theory is that molecular interaction forces do not appear explicitly but instead all necessary information is carried by the pair correlation function, also known as radial distribution function, of an inhomogeneous fluid. Evidently one must use additional theoretical or computational models to obtain information on this function, a task that is not always easy to accomplish [9,10].

Over the past two decades, the continuous development of more rigorous molecular or atomistic models of liquid-vapor systems, in conjunction with the dramatic improvement in computational power, has resulted in a more in-depth understanding of the underlying physics of these systems. Traditional computational fluid dynamics methods have many difficulties and limitations in this area, while molecular simulation models have excessively large computational requirements for the solution of even relatively simple problems, and are limited to extremely small time and/or space scales and simple geometries. In this context, the use of the lattice Boltzmann equation (LBE) method to study multiphase equilibrium and transport processes has increased significantly over the last decade.

The LBE method is a mesoscopic approach that incorporates microscopic physics at a reasonable computational expense [11–13]. Even though the major focus of the method has been on averaged macroscopic behavior, its kinetic nature can provide many of the advantages of molecular dynamics, bridging the gap between molecular simulations at the microscopic level and simulations based on macroscopic conservation laws [14]. The method is especially useful for complex systems in which the macroscopic governing equations cannot be determined in a straightforward manner while microscopic physics is adequately described to a cer-

tain level of approximation. Several approaches exist for modeling liquid-vapor fluids using the LBE method (see for example [13,14] and references cited therein). In the present study we focus on the so called forcing method, which is guided by an atomistic formalism where interparticle interactions are introduced by the direct introduction of a forcing term in the LB equation [15–20]. It has been previously recognized that this approach leads to a nonideal equation of state that can produce phase separation [16].

A major breakthrough in the LBE theory has been the direct derivation of the LBE from the continuous Boltzmann equation under certain conditions [21,22]. The successful establishment of the theoretical foundation for the LBE method in the framework of kinetic theory of gases has led to more rigorous ways of incorporating molecular interactions in the LBE following the BBGKY formalism [23–25] and/or Enskog’s extension of Boltzmann’s equation [23,26–29]. In their original work, He *et al.* [26] introduced a forcing term considering interparticle interaction using a mean-field treatment in the same way that the Coulomb interaction among the charged particles of a plasma is treated in Vlasov’s equation [26,30]. Later, He and Doolen [23] improved the above model starting from the BBGKY equations and established the thermodynamic foundations of the LB multiphase models by showing that a kinetic equation that combines Enskog’s theory for dense fluids and the mean-field theory for long-range molecular interaction can consistently describe non-ideal gases and dense fluid flows. Luo [27,28] carried out a systematic derivation of a thermodynamically consistent LBE model for nonideal gases starting from the Enskog equation. In all the above cases the basic features of the Van der Waals theory are retained and set the thermodynamic limits of the validity of these models.

Based on the approach of He *et al.* [26] and later He and Doolen [23], several LBE models have been proposed using either Lagrangian [31] or Eulerian-based finite difference schemes [32] for the discretization of the convective (advection) terms. However, in many cases these models failed to provide accurate predictions for the bulk and interfacial thermodynamic properties [33].

Lee and Lin [34] and later Lee and Fischer [35] have developed LBE models that employ the chemical potential instead of the pressure gradient as the driving force, through the Gibbs-Duhem equation. Furthermore, these authors have used alternative numerical schemes for the discretization of the directional derivatives of the LBE model and their results have shown an improved stability and accuracy for large density differences, using a simplified equation of state, during static and dynamic conditions. More recently Kikkinides *et al.* [36] have demonstrated that the Gibbs-Duhem based LBE model with the numerical scheme proposed by Lee and Fischer is thermodynamically consistent in the sense that it can recover accurately both bulk and interface thermodynamic properties for several equations of state. Furthermore it has been recently demonstrated that the Gibbs-Duhem based LBE model can describe accurately complex multiphase flows including low Weber droplet flow and Rayleigh-Taylor instability without exhibiting parasitic currents that were previously observed [37].

The limitation of all LBE multiphase models proposed so far is that they require an equation of state, which in most

cases is empirical or semiempirical in nature. In many cases several interparticle potentials have been applied to obtain a suitable equation of state [38,39], while in other cases multi-range interaction models have been proposed to control the surface tension independently of the equation of state [20,40]. In either case none of these potentials can be related to fundamental interaction potentials that are based on statistical thermodynamics.

Martys [24], on the other hand, has proposed an alternative route to model the force in the LBE model using a density gradient expansion of the BBGKY collision operator, in accord with the mechanical approach of gradient theory [6,7]. The advantage of this approach is that the force term is no longer related to an equation of state but instead it contains information related to the molecular interaction potential both explicitly and implicitly, through the radial distribution function. This approach, although very promising, since it relates for the first time the force term in the LBE model directly to a fundamental property from statistical mechanics, has not been explored so far, mainly due to the assumption that the radial distribution function does not depend on the fluid density [24]. An alternative methodology that relates the forcing term directly to the molecular interaction potential has been recently proposed and is based on principles from density functional theory (DFT) [41]. This approach is also expected to give important physical insight on the interface characteristics of complex fluids in the near future.

In the present study, we extend and generalize Martys’ work by developing an LBE model that is based on the density gradient expansion of the discrete BBGKY evolution equations. In the proposed model, the basic input is the radial distribution function that is related exclusively to the molecular interaction potential. This function is provided from independent molecular simulations or from approximate theories. The discretization strategy is based on Lee-Fischer’s work [35], since it has been shown that this method gives thermodynamically consistent models and negligible parasitic currents [36].

We have applied our proposed model to obtain bulk and interfacial equilibrium properties including molar densities, equilibrium pressure and surface tension for a Lennard-Jones (LJ) fluid at different temperatures relatively close to the critical temperature. The majority of the simulations are performed for the case of a planar interface, nevertheless curved (circular) interfaces have also been considered to validate Laplace’s law and compare the interfacial properties of the fluid for both interface geometries.

## II. MODEL DEVELOPMENT

A rigorous way to derive a consistent LBE method for nonideal gases is to start from the basic equation of nonequilibrium statistical mechanics, which is the Liouville equation for a gas with pair interactions [42]. Accordingly, we employ the BBGKY hierarchy of equations for the various distribution functions. These equations describe the dependence of the time evolution of a  $n$  particle distribution function expressed in terms of a  $n+1$  particle distribution function. Fol-

lowing [42,43], the BBGKY equations for the first or single distribution function, assuming pairwise interactions, is written as

$$\frac{\partial f_1}{\partial t} + \boldsymbol{\xi}_1 \cdot \frac{\partial f_1}{\partial \mathbf{r}_1} + \frac{\mathbf{F}_e}{m} \cdot \frac{\partial f_1}{\partial \boldsymbol{\xi}_1} + \frac{1}{m} \int \int \frac{\partial f_{12}}{\partial \boldsymbol{\xi}_1} \cdot \frac{\partial V(|\mathbf{r}_{12}|)}{\partial \mathbf{r}_1} d\boldsymbol{\xi}_2 d\mathbf{r}_2 = 0, \quad (1)$$

where  $f_1=f_1(\mathbf{r}_1, \boldsymbol{\xi}_1, t)$  is the single particle distribution function,  $f_{12}=f_{12}(\mathbf{r}_1, \boldsymbol{\xi}_1, \mathbf{r}_2, \boldsymbol{\xi}_2, t)$  is the two particle distribution function,  $m$  is the particle mass, and  $\mathbf{r}_i, \boldsymbol{\xi}_i$  ( $i=1,2$ ) are the position and microscopic velocity vectors of the particles, respectively.  $V$  is the interparticle potential,  $\mathbf{r}_{12}=\mathbf{r}_2-\mathbf{r}_1$ , and  $\mathbf{F}_e$  is the external force. For the case of a Lennard-Jones (LJ) fluid the interparticle potential is given by the well known expression,

$$V(r) = 4\varepsilon \left[ \left( \frac{\sigma}{r} \right)^{12} - \left( \frac{\sigma}{r} \right)^6 \right], \quad (2)$$

where  $\sigma$  is the collision (molecular) diameter and  $\varepsilon$  is the depth of the potential well at the minimum of  $V(r)$ . The Lennard-Jones potential provides a fair description of the interaction between pairs of rare-gas atoms and also of quasi-spherical molecules such as methane.

Introducing the operators

$$S_1 = \frac{\partial}{\partial t} + \boldsymbol{\xi}_1 \cdot \frac{\partial}{\partial \mathbf{r}_1} + \frac{\mathbf{F}_e}{m} \cdot \frac{\partial}{\partial \boldsymbol{\xi}_1}, \quad (3a)$$

$$\Omega_1 = -\frac{1}{m} \int \int \frac{\partial V(|\mathbf{r}_{12}|)}{\partial \mathbf{r}_1} \cdot \frac{\partial}{\partial \boldsymbol{\xi}_1} d\boldsymbol{\xi}_2 d\mathbf{r}_2, \quad (3b)$$

Eq. (1) becomes

$$S_1\{f_1\} = \Omega_1\{f_{12}\}. \quad (4)$$

It is seen that we cannot solve Eqs. (1) or (4) for  $f_1$  since the variable  $f_{12}$  is also unknown. Evidently the BBGKY equations are not independent since the  $n$ th equation contains the  $(n+1)$  unknown particle distribution function each time. Therefore we need to impose some closure hypothesis to carry on with a formal solution. Following the closure hypothesis for the Vlasov-Bhatnagar-Gross-Krook equation we have [43]

$$f_{12}(\mathbf{r}_1, \boldsymbol{\xi}_1, \mathbf{r}_2, \boldsymbol{\xi}_2, t) = f_1(\mathbf{r}_1, \boldsymbol{\xi}_1, t) f_1(\mathbf{r}_2, \boldsymbol{\xi}_2, t) g^{eq}(\mathbf{r}_1, \mathbf{r}_2) + \chi_{12}, \quad (5)$$

where  $g^{eq}(\mathbf{r}_1, \mathbf{r}_2)$  is the radial distribution function at equilibrium and  $\chi_{12}$  designates the difference between  $f_{12}$  and  $f_1(\mathbf{r}_1, \boldsymbol{\xi}_1, t) f_1(\mathbf{r}_2, \boldsymbol{\xi}_2, t) g^{eq}(\mathbf{r}_1, \mathbf{r}_2)$  away from equilibrium.

Introducing the Bhatnagar-Gross-Krook (BGK) hypothesis in the right-hand term of Eq. (4) leads to [43]

$$\begin{aligned} \Omega_1\{f_{12}\} &= \Omega_1\{f_1(\mathbf{r}_1, \boldsymbol{\xi}_1, t) f_1(\mathbf{r}_2, \boldsymbol{\xi}_2, t) g^{eq}(\mathbf{r}_1, \mathbf{r}_2)\} + \Omega_1\{\chi_{12}\} \\ &= \Omega_1\{f_1(\mathbf{r}_1, \boldsymbol{\xi}_1, t) f_1(\mathbf{r}_2, \boldsymbol{\xi}_2, t) g^{eq}(\mathbf{r}_1, \mathbf{r}_2)\} \\ &\quad + \frac{f_1^{eq}(\mathbf{r}_1, \boldsymbol{\xi}_1) - f_1(\mathbf{r}_1, \boldsymbol{\xi}_1, t)}{\lambda}. \end{aligned} \quad (6)$$

Then after some straightforward manipulations [given that  $\int \boldsymbol{\xi}_2 f_1(\mathbf{r}_2, \boldsymbol{\xi}_2, t) d\boldsymbol{\xi}_2 = \rho(\mathbf{r}_2, t)$ ], Eq. (4) is written in the following form:

$$\begin{aligned} \frac{\partial f_1}{\partial t} + \boldsymbol{\xi}_1 \cdot \frac{\partial f_1}{\partial \mathbf{r}_1} + \frac{\mathbf{F}_e}{m} \cdot \frac{\partial f_1}{\partial \boldsymbol{\xi}_1} \\ = -\frac{1}{m} \frac{\partial f_1}{\partial \boldsymbol{\xi}_1} \cdot \int \frac{\partial V(|\mathbf{r}_{12}|)}{\partial \mathbf{r}_1} \rho(\mathbf{r}_2) g^{eq}(\mathbf{r}_1, \mathbf{r}_2) d\mathbf{r}_2 + \frac{f_1^{eq} - f_1}{\lambda}. \end{aligned} \quad (7)$$

The above equation is very similar to the ones proposed earlier [23–25] and describes the evolution of the single particle distribution function for a dense fluid following the BBGKY hierarchy and the BGK hypothesis for the type of the particle collisions. The difference between Eq. (7) and the one proposed by Martys [24], is the current inclusion of a BGK relaxation term for the one-body collisions. This term is responsible for the transition to equilibrium and is not related to the equilibrium properties of the fluid. The parameter  $\lambda$  in the denominator of the BGK-term is a phenomenological mean collision time parameter, which can be directly related to the viscosity of the fluid [41]. A similar term appears in related studies [25,44,41].

We continue our analysis by neglecting any external force ( $\mathbf{F}_e=0$ ) and letting  $\mathbf{r}_2=\mathbf{r}_1+\mathbf{r}$ . Then Eq. (7) is written as

$$\begin{aligned} \frac{\partial f_1}{\partial t} + \boldsymbol{\xi}_1 \cdot \frac{\partial f_1}{\partial \mathbf{r}_1} = -\frac{1}{m} \frac{\partial f_1}{\partial \boldsymbol{\xi}_1} \cdot \left[ \int \rho(\mathbf{r}_1 + \mathbf{r}) g^{eq}(\mathbf{r}_1, \mathbf{r}_1 + \mathbf{r}) \right. \\ \left. \times \left( \frac{\partial V(r)}{\partial r} \frac{\mathbf{r}}{r} \right) d^3 r \right] + \frac{(f_1^{eq} - f_1)}{\lambda} \end{aligned} \quad (8)$$

or

$$\frac{\partial f_1}{\partial t} + \boldsymbol{\xi}_1 \cdot \frac{\partial f_1}{\partial \mathbf{r}_1} = -\frac{1}{m} \frac{\partial f_1}{\partial \boldsymbol{\xi}_1} \cdot I + \frac{(f_1^{eq} - f_1)}{\lambda}, \quad (9)$$

where

$$I = \int \rho(\mathbf{r}_2) g^{eq}(\mathbf{r}_1, \mathbf{r}_2) \left( \frac{\partial V(r)}{\partial r} \frac{\mathbf{r}}{r} \right) d^3 r. \quad (10)$$

### A. Gradient approximation

Equation (8) is still not very useful to obtain a solution for the distribution function in time and space since the integral in the right-hand side is not easily solvable. Nevertheless, there have been a few attempts to solve the above equation either under very specific conditions and assumptions (see for example [25]) or using elements of DFT [41].

A different approach involves the application of density gradient approximation, where we expand density and its functions around  $\mathbf{r}_1$  using Taylor expansions to obtain differential equations that are solvable under certain conditions. The density gradient approximation has imbedded in it the assumption of slowly varying properties around  $\mathbf{r}_1$ , a condition that is met only in the immediate vicinity of the critical temperature,  $T_c$ , for a fluid. Nevertheless, experience has shown that this approximation remains valid even for  $T/T_c$

down to 0.9. Davis, Scriven and co-workers [5–8] have performed in the past extensive studies to come up with useful formulations that can be employed to study interface properties using gradient theory. Thus we focus on expanding the integral  $I$  in the right-hand side of Eq. (10) in terms of density gradients in accord with the above theory.

Following [7], we expand  $\rho(\mathbf{r}_2)=\rho(\mathbf{r}_1+\mathbf{r})$  around  $\mathbf{r}_1$  with respect to  $\mathbf{r}$ , keeping up to 3rd order gradients to get

$$\rho(\mathbf{r}_2) = \rho(\mathbf{r}_1) + \mathbf{r} \cdot \nabla \rho_1 + \frac{1}{2} \mathbf{r} \mathbf{r} : \nabla \nabla \rho_1 + \frac{1}{6} \mathbf{r} \mathbf{r} \mathbf{r} : \nabla \nabla \nabla \rho_1, \quad (11)$$

where we have used the notation:  $\rho_i = \rho(\mathbf{r}_i)$ , for  $i=1,2$ .

To continue our procedure we must make an elementary hypothesis on the structure of the pair correlation function, of an inhomogeneous fluid,  $g^{eq}(\mathbf{r}_1, \mathbf{r}_2)$ , with that of a homogeneous fluid at some local density or densities. Since  $g^{eq}(\mathbf{r}_1, \mathbf{r}_2)$  appears in Eqs. (8) or (10) as a product with the intermolecular force, it can be argued that only configurations for which the particles are close to each other contribute appreciably to the theory [6]. Thus pair correlations can be determined as those of a homogeneous fluid at a density in the neighborhood of the correlated particles. The three most common choices for such an approximation are [6–8], (a) density at the mean location,  $\bar{\mathbf{r}}=(\mathbf{r}_1+\mathbf{r}_2)/2$ , (b) mean density  $\bar{\rho}=(\rho_1+\rho_2)/2$ , or (c) mean pair correlation function,  $\frac{1}{2}[g^{eq}(\mathbf{r};\rho_1)+g^{eq}(\mathbf{r};\rho_2)]$ , where again,  $\rho_i=\rho(\mathbf{r}_i)$ , for  $i=1,2$ .

In any of these choices an important approximation is made regarding the absence of transverse correlations which can be important close to the interface. Rigorous theory on the other hand has shown that transverse correlations, which are gradient-induced, are in general not zero [1,6,45]. Nevertheless, it has been demonstrated that, for a 6–12 LJ fluid, the density profiles and surface tensions predicted by any of the above local density approximations are in very good agreement with those predicted by exact gradient theory [8]. This implies that the neglected correlations do not contribute strongly to the fluid tension [6,45], at least in the neighborhood of the critical temperature,  $T_c$ .

In the present study we have considered choice (c); thus it follows that

$$\begin{aligned} g^{eq}(\mathbf{r}_1, \mathbf{r}_2) &= g^{eq}(\mathbf{r}_1, \mathbf{r}_1 + \mathbf{r}) \\ &\cong \frac{1}{2}[g^{eq}(\mathbf{r};\rho_1) + g^{eq}(\mathbf{r};\rho_2)]. \end{aligned} \quad (12)$$

Expanding  $g(\mathbf{r};\rho_2)$  up to third order terms we get

$$\begin{aligned} g^{eq}(\mathbf{r};\rho_2) &= g^{eq}(\mathbf{r};\rho_1) + \left(\frac{\partial g^{eq}}{\partial \rho}\right)_1 (\rho_2 - \rho_1) + \frac{1}{2} \left(\frac{\partial^2 g^{eq}}{\partial \rho^2}\right)_1 (\rho_2 - \rho_1)^2 \\ &\quad + \frac{1}{6} \left(\frac{\partial^3 g^{eq}}{\partial \rho^3}\right)_1 (\rho_2 - \rho_1)^3. \end{aligned} \quad (13)$$

Substituting Eqs. (11)–(13) in Eq. (10), the latter becomes

$$\begin{aligned} I &= \int \left\{ \left[ \rho(\mathbf{r}_1) + \mathbf{r} \cdot \nabla \rho_1 + \frac{1}{2} \mathbf{r} \mathbf{r} : \nabla \nabla \rho_1 + \frac{1}{6} \mathbf{r} \mathbf{r} \mathbf{r} : \nabla \nabla \nabla \rho_1 \right] \right. \\ &\quad \times \left[ g^{eq}(\mathbf{r};\rho_1) + \frac{1}{2} \left(\frac{\partial g^{eq}}{\partial \rho}\right)_1 (\rho_2 - \rho_1) + \frac{1}{4} \left(\frac{\partial^2 g^{eq}}{\partial \rho^2}\right)_1 (\rho_2 - \rho_1)^2 \right. \\ &\quad \left. \left. + \frac{1}{12} \left(\frac{\partial^3 g^{eq}}{\partial \rho^3}\right)_1 (\rho_2 - \rho_1)^3 \right] \left( \frac{\partial V(r) \mathbf{r}}{\partial r} \right) d^3 r \right\}, \end{aligned} \quad (14)$$

where  $\rho_2 - \rho_1$  in Eq. (14) is determined by Eq. (11) above. The integral in Eq. (14) requires tedious operations keeping terms up to third order in gradients of  $\rho$ . Such an approach is cumbersome even in 1D and some additional assumptions must be made to proceed and come up with practically useful and tractable expressions.

For the 1D case and after a series of calculations, it can be shown that the above equation becomes

$$\begin{aligned} I &= -a \frac{d\rho}{dx} - \frac{1}{2} \rho \frac{da}{dx} + \left( \frac{u_2}{2} + \frac{\rho du_2}{4 d\rho} \right) \frac{d^3 \rho}{dx^3} + \left( \frac{3 du_2}{2 d\rho} \right. \\ &\quad \left. + \frac{3 d^2 u_2}{4 d\rho^2} \right) \frac{d\rho d^2 \rho}{dx dx^2} + \left( \frac{3 d^2 u_2}{4 d\rho^2} + \frac{\rho d^3 u_2}{4 d\rho^3} \right) \left( \frac{d\rho}{dx} \right)^3, \end{aligned} \quad (15)$$

where parameters  $a$ ,  $u_2$  are the first and third moments of force [7], and are defined as follows:

$$a = -\frac{4\pi}{3} \int_0^\infty g^{eq}(r;\rho) \frac{\partial V(r)}{\partial r} r^3 dr, \quad (16)$$

$$u_2 = \frac{4\pi}{15} \int_0^\infty g^{eq}(r;\rho) \frac{\partial V(r)}{\partial r} r^5 dr. \quad (17)$$

Note that in the above equations subscript 1 has been omitted for simplicity, in accord with similar studies [7,23,24].

The above equation is still cumbersome to employ in the LBM model. Moreover, it was shown before that unless we assume that the third moment of force,  $u_2$ , does not depend on density,  $\rho$ , the gradient approximation of the mechanical theory is not consistent with the van der Waals, Cahn, Hilliard (vdW-CH) thermodynamic theory [6,7,46]. Fortunately  $u_2$  is indeed a weak function of density at least in the phase transition region and at  $0.9 < T/T_c < 1$ , which is the region where the gradient theory holds anyway (McCoy *et al.* [8]).

Thus, if we assume that  $\frac{d^i u_2}{d\rho^i} \approx 0$ , for  $i \geq 1$ , Eq. (15) becomes

$$I = -a \frac{d\rho}{dx} - \frac{1}{2} \rho \frac{da}{dx} + \left( \frac{u_2}{2} \right) \frac{d^3 \rho}{dx^3}. \quad (18)$$

With the above assumptions it is straightforward to show that the above expression becomes in 3D,

$$I = -a \nabla \rho - \frac{1}{2} \rho \nabla a + \left( \frac{u_2}{2} \right) \nabla \nabla^2 \rho. \quad (19)$$

Substituting Eq. (19) in Eq. (9) the latter becomes (again omitting subscript 1),

$$\frac{\partial f}{\partial t} + \xi \cdot \frac{\partial f}{\partial \mathbf{r}} = -\frac{1}{m} \frac{\partial f}{\partial \xi} \cdot \left\{ -a \nabla \rho - \frac{1}{2} \rho \nabla a + \left( \frac{u_2}{2} \right) \nabla \nabla^2 \rho \right\} + \frac{(f^{eq} - f)}{\lambda}. \quad (20)$$

Assuming that  $f$  is close to  $f^{eq}$ , which corresponds to a Maxwellian gas, we have

$$f^{eq} = \rho \left( \frac{m}{2\pi k_B T} \right)^{3/2} \exp \left[ -\frac{m(\xi - \mathbf{u})^2}{2k_B T} \right]. \quad (21)$$

Then we can write that [23]

$$\frac{\partial f}{\partial \xi} \approx \frac{\partial f^{eq}}{\partial \xi} = -\frac{m(\xi - \mathbf{u})}{k_B T} f^{eq} = -\frac{\rho m(\xi - \mathbf{u})}{\rho k_B T} f^{eq}. \quad (22)$$

Substituting Eq. (22) into Eq. (20), the latter becomes

$$\frac{\partial f}{\partial t} + \xi \cdot \frac{\partial f}{\partial \mathbf{r}} = \frac{(\xi - \mathbf{u})}{\rho k_B T} f^{eq} \cdot \left\{ -a \rho \nabla \rho - \frac{1}{2} \rho^2 \nabla a + \rho \left( \frac{u_2}{2} \right) \nabla \nabla^2 \rho \right\} + \frac{(f^{eq} - f)}{\lambda} \quad (23)$$

or

$$\frac{\partial f}{\partial t} + \xi \cdot \frac{\partial f}{\partial \mathbf{r}} = \frac{(\xi - \mathbf{u})}{\rho k_B T} f^{eq} \cdot \left\{ \nabla \left( -\frac{a\rho^2}{2} \right) + \rho \kappa \nabla \nabla^2 \rho \right\} + \frac{(f^{eq} - f)}{\lambda}, \quad (24)$$

where parameter  $\kappa = u_2/2$  is the well known influence parameter of gradient theory and is a measure of the magnitude of surface tension at the microscopic level.

Note that the forcing term in the brackets of the right-hand side of Eq. (24) is practically identical to the one derived by Martys [24]. However, in his model derivation Martys has assumed that the radial distribution function does not depend on density and as a result both parameters  $a$  and  $\kappa$  are constant, while in the present study  $a$  can vary with  $\rho$ .

From statistical thermodynamics [9,10], it has been shown that the general form of an equation of state for any fluid with spherical potential and pair interactions is

$$P_0 = \rho k_B T - \frac{2\pi\rho^2}{3} \left[ \int_0^\infty g^{eq}(r; \rho) \frac{\partial V(r)}{\partial r} r^3 dr \right], \quad (25)$$

where  $P_0$  is the bulk pressure of the fluid. The above equation is a general equation of state, where the first term in the right-hand side is the ideal gas law term while the second term shows the deviation of a fluid from the ideal gas law. Based on the definition of the first moment of force,  $a$ , [Eq. (16)] the above equation becomes

$$P_0 = \rho k_B T + \frac{a\rho^2}{2}. \quad (26)$$

Combining Eq. (26) with Eq. (24), the latter becomes

$$\frac{\partial f}{\partial t} + \xi \cdot \frac{\partial f}{\partial \mathbf{r}} = \frac{(\xi - \mathbf{u})}{\rho k_B T} f^e \cdot [\nabla(\rho k_B T) - \nabla P_0 + \kappa \rho \nabla \nabla^2 \rho] + \frac{(f^e - f)}{\lambda}. \quad (27)$$

Employing the Gibbs-Duhem equation for the bulk pressure, Eq. (27) becomes

$$\frac{\partial f}{\partial t} + \xi \cdot \frac{\partial f}{\partial \mathbf{r}} = \frac{(\xi - \mathbf{u})}{\rho k_B T} f^e \cdot [\nabla(\rho k_B T) - \rho \nabla \mu] + \frac{(f^e - f)}{\lambda}, \quad (28)$$

where

$$\mu = \mu_0 - \kappa \nabla^2 \rho \quad (29)$$

in accord with Van der Waals theory and its successors. The bulk chemical potential  $\mu_0$  for a fluid that obeys the general equation of state Eq. (26) is found by solving the equation for the bulk free energy density  $F_0$ ,

$$P_0 = \rho \mu_0 - F_0 \quad \text{where} \quad \mu_0 = \frac{\partial F_0}{\partial \rho}. \quad (30)$$

Solving Eq. (30) with the aid of Eq. (26) (see [35]), we get the following expression for  $\mu_0$ :

$$\mu_0 = \mu_0^+ + k_B T (\ln \rho / \rho_0 + 1) + \int_{\rho_0}^{\rho} \frac{a}{2} d\rho' + \frac{a}{2} \rho, \quad (31)$$

where  $\mu_0^+$  is a constant of integration that depends on temperature,  $T$ , and  $\rho_0$  is a reference density that can be the equilibrium density of either gas or liquid phase. Note that the selection of these parameters does not affect the simulations since it is the gradient of the chemical potential that matters and not its exact value. Thus, in the present case we work with the chemical potential difference,  $\Delta\mu_0 = \mu_0 - \mu_0^+$ , and  $\rho_0 = \rho_g$ .

Equation (28) is identical with previously developed LBE models [35,36], but with two important differences: (a) the expressions for bulk chemical potential and pressure are given for the general equation of state that relates these variables with the intermolecular potential of the fluid, and (b) parameters  $a$  and  $\kappa$  are calculated from different expressions compared to previous studies, in accord with Martys's work [24]. Note that for a constant value of the third moment of force,  $u_2$ , the three suggested choices of the local density approximations of the radial distribution function described above, become identical [7].

The numerical implementation of the model can be done in exactly the same way as in [35,36], provided that we have direct information on the intermolecular potential and the radial distribution function, which constitute the main input parameters to the present LBE model. Since this analysis have been done in detail elsewhere [35,36] we provide only the salient features of this method in the present study.

Following Lee and Fischer [35], Eq. (28) is discretized as follows:

$$\begin{aligned} \bar{f}_i(\mathbf{x} + \boldsymbol{\xi}_i \delta t, t + \delta t) - \bar{f}_i(\mathbf{x}, t) = & - \left[ \frac{1}{\tau + 0.5} (\bar{f}_i - \bar{f}_i^{eq}) \right]_{\mathbf{x}, t} \\ & + \frac{(\boldsymbol{\xi}_i - \mathbf{u})(\nabla^M \rho k_B T - \rho \nabla^M \mu)}{\rho k_B T} \\ & \times f_i^{eq}(\mathbf{x}, t) \delta t, \end{aligned} \quad (32)$$

where

$$\bar{f}_i^{eq} = f_i^{eq} - \frac{\delta t (\boldsymbol{\xi}_i - \mathbf{u})(\nabla^C \rho k_B T - \rho \nabla^C \mu)}{2 \rho k_B T} f_i^{eq}. \quad (33)$$

The equilibrium distribution function  $f_i^{eq}$  is given by the well known expression [following a Taylor expansion of Eq. (21)],

$$f_i^{eq} = w_i \rho \left[ 1 + \frac{\boldsymbol{\xi}_i \cdot \mathbf{u}}{RT} + \frac{(\boldsymbol{\xi}_i \cdot \mathbf{u})^2}{2(RT)^2} - \frac{(\mathbf{u} \cdot \mathbf{u})}{2RT} \right], \quad i = 0, N_b - 1, \quad (34)$$

where  $w_i$  is a weighting factor that depends on the lattice type used in the LBE model,  $N_b$  is the number of bonds emanating from each lattice site and  $i$  is the index of each velocity bond (for the D2Q9 LB-model  $N_b=9$ , and so on).

Gradients of density are discretized by the following mixed scheme [35],

$$\nabla^M \rho|_{(\mathbf{x})} = \frac{1}{2} [\nabla^C \rho|_{(\mathbf{x})} + \nabla^B \rho|_{(\mathbf{x})}], \quad (35a)$$

$$\delta t \boldsymbol{\xi}_i \cdot \nabla^M \rho|_{(\mathbf{x})} = \frac{1}{2} [\delta t \boldsymbol{\xi}_i \nabla^C \rho|_{(\mathbf{x})} + \delta t \boldsymbol{\xi}_i \nabla^B \rho|_{(\mathbf{x})}]. \quad (35b)$$

Note that parameter  $\tau$  in Eq. (32), is the modified collision time employed in the discretized form of the LBE [11,12,35].

The above mixed scheme considers an equal contribution of central (superscript  $C$ ) and biased (superscript  $B$ ) finite differences. For the case of directional derivatives the following second order schemes are used for central and biased differences, respectively,

$$\delta t \boldsymbol{\xi}_i \cdot \nabla^C \rho|_{(\mathbf{x})} = \frac{\rho(\mathbf{x} + \boldsymbol{\xi}_i \delta t) - \rho(\mathbf{x} - \boldsymbol{\xi}_i \delta t)}{2}, \quad (36a)$$

$$\delta t \boldsymbol{\xi}_i \cdot \nabla^B \rho|_{(\mathbf{x})} = \frac{-\rho(\mathbf{x} + 2\boldsymbol{\xi}_i \delta t) + 4\rho(\mathbf{x} + \boldsymbol{\xi}_i \delta t) - 3\rho(\mathbf{x})}{2}. \quad (36b)$$

Derivatives other than directional are computed by taking moments of the 1D finite difference schemes with appropriate weights to yield isotropic discretizations [35,36],

$$\nabla^C \rho|_{(\mathbf{x})} = \sum_{i \neq 0} \frac{w_i \boldsymbol{\xi}_i [\rho(\mathbf{x} + \boldsymbol{\xi}_i \delta t) - \rho(\mathbf{x} - \boldsymbol{\xi}_i \delta t)]}{2k_B T \delta t}, \quad (37a)$$

$$\nabla^B \rho|_{(\mathbf{x})} = \sum_{i \neq 0} \frac{w_i \boldsymbol{\xi}_i [-\rho(\mathbf{x} + 2\boldsymbol{\xi}_i \delta t) + 4\rho(\mathbf{x} + \boldsymbol{\xi}_i \delta t) - 3\rho(\mathbf{x})]}{2k_B T \delta t}, \quad (37b)$$

$$\nabla^2 \rho|_{(\mathbf{x})} = \sum_{i \neq 0} \frac{w_i [\rho(\mathbf{x} + \boldsymbol{\xi}_i \delta t) - 2\rho(\mathbf{x}) + \rho(\mathbf{x} - \boldsymbol{\xi}_i \delta t)]}{k_B T \delta t^2}. \quad (37c)$$

Accordingly, density and velocity vector are determined taking the moments of the distribution function resulting in the following expressions:

$$\rho = \sum_i \bar{f}_i, \quad (38)$$

$$\mathbf{u} = \sum_i \bar{f}_i \boldsymbol{\xi}_i / \rho + \frac{\delta t}{2} (\nabla^C \rho k_B T - \rho \nabla^C \mu). \quad (39)$$

Further details of the above discretization method are given in [35,36].

### B. Determination of the radial distribution function

The radial distribution function  $g^{eq}(r; \rho)$ , which physically represents the structure of a fluid, acts as a bridge for relating macroscopic thermodynamic properties to microscopic molecular interactions in a fluid. This function is a key quantity in statistical mechanics since it describes quantitatively how the intermolecular correlations in a fluid decay with increasing separation,  $r$ , at different bulk fluid densities,  $\rho$ . Its formal definition is through the product  $\rho g^{eq}(r; \rho)$ , which is the average density of atoms at a distance  $r$ , given that another atom is located at the origin [10]. At large separations  $g^{eq}(r; \rho) = 1$ . For gases at low densities the radial distribution function is equal to the Boltzmann factor of the pair potential [9,10],

$$\lim_{\rho \rightarrow 0} g(r; \rho) = \exp \left[ - \frac{V(r)}{k_B T} \right]. \quad (40)$$

From the above equation it is easy to conclude that the non-ideal gas term in the general equation of state [Eq. (26)] vanishes at high temperatures and low densities for a LJ fluid.

There are numerous approaches to determine  $g^{eq}(r; \rho)$  in the whole density range. For this reason various methods of obtaining this function have been introduced:

(a) Perturbation theories including the well known Barker-Henderson (BH) and Weeks-Chandler-Anderson (WCA) theories and their extensions (for a review on these and related theories see for example [9,10] and references cited therein). These methods describe a LJ fluid fairly well beyond low densities. In addition, a number of integral-equation theories such as the Percus-Yevick (PY), the hypernetted chain (HNC) and other recently developed approximations toward solving the Ornstein-Zernike (OZ) equation are adopted to study the LJ fluid (see [9,10,47] and references cited therein). All the above theories are approximate in nature and fail to describe accurately the liquid-vapor equilibrium properties of a LJ fluid at  $T_r = T/T_c > 0.9$ . Moreover, some of the above theories require tedious calculations which limit parts of their original advantages.

(b) Computer simulation methods (molecular dynamics or Monte Carlo) [48]. These are more rigorous methods that are used to predict equilibrium and some times dynamic properties of a fluid. Molecular dynamics solve Newton's laws for

a large number of molecules interacting through an intermolecular potential. Monte Carlo methods are less rigorous and are based on the use of Metropolis algorithm employed to minimize the free energy of a system of a large number of molecules interacting again with a LJ potential with pair interactions. Both methods work well at all conditions, however extra care must be taken when working near the critical temperature where long-range correlations become significant requiring more particles and larger equilibration times in the simulations [49,50].

(c) There are also experimental methods (see for example [10] and references cited therein), however there are several complications associated with them.

In the present work molecular dynamics (MD) have been employed for the calculation of  $g^{eq}(r; \rho)$ . The molecules interact with each other through a LJ potential assuming pairwise interactions to comply with the assumptions of the present LBE model. The resulting radial distribution functions as functions of distance have been tabulated for each density and temperature. Accordingly, for a certain temperature we can use interpolation formulas to get  $g^{eq}(r; \rho)$  for any value of  $r, \rho$  in the integral, provided that our interpolation region contains these values. Fine space resolution has been imposed (1000 points for  $0 < r < 8.8\sigma$ ) to minimize artifacts during interpolation.

We obtain  $g^{eq}(r; \rho)$  from MD at equilibrium using a standard open-source software (MOLDY) [51]. The advantage of this approach is that we only need the interaction potential as an input and not a semiempirical (and often inaccurate) equation of state. The basic assumption is that only pair interactions must be included in the simulation to comply with the gradient theory-based model derivation. In all simulations we have used 10 000–12 000 spherical molecules per run while long equilibration times have been employed to ensure that we have reached equilibrium conditions [typically of the order of  $2 \times 10^5$  time steps or more, with a time step,  $\delta t = 2.32 \times 10^{-3} \sigma (\frac{m}{\epsilon})^{1/2}$ ]. The density spectrum ranged for dimensionless densities,  $\rho^* = \rho \sigma^3$ , from 0.05 up to 0.8 and for dimensionless temperatures,  $T^* = k_B T / \epsilon$ , ranging from 1.2 up to 1.27. At dimensionless densities below 0.05, the low density analytical expression [Eq. (40)] has been employed. The cutoff radius is set  $5.87\sigma$  to account for long-range correlations, as it has been demonstrated that this limit produces accurate vapor-liquid equilibrium data even close to the critical temperature [49]. Note that the information on  $g^{eq}(r; \rho)$  is provided from the MD simulation package for distances up to  $8.8\sigma$ . Beyond this distance we set  $g^{eq}(r; \rho) = 1$ .

Finally, in order to solve the LBE model equations we have expressed them in dimensionless form using the following dimensionless variables:  $T^* = k_B T / \epsilon$ ,  $\rho^* = \rho \sigma^3$ ,  $\mathbf{P}^* = \mathbf{P} \sigma^3 / \epsilon$ ,  $\mu_0^* = \mu_0 / \epsilon$ ,  $\gamma^* = \gamma \sigma^2 / \epsilon$ ,  $r^* = r / \sigma$ ,  $x^* = x / \sigma$ ,  $a^* = a / \epsilon \sigma^3$ ,  $\kappa^* = \kappa / \epsilon \sigma^5$ ,  $t^* = t (\frac{\epsilon}{m \sigma^2})^{1/2}$ ,  $\lambda^* = \lambda (\frac{\epsilon}{m \sigma^2})^{1/2}$ .

### III. RESULTS AND DISCUSSION

#### A. Determination of vapor-liquid equilibrium properties

##### 1. Maxwell construction

A series of MD simulations have been performed at fixed temperature, for a certain density range in order to determine

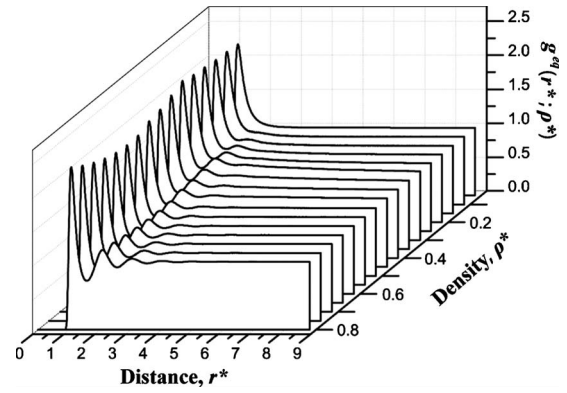


FIG. 1. Radial distribution functions at different densities,  $T^* = 1.25$ .

the respective radial distribution function (RDF) at each temperature. A typical plot of RDF's at different densities is presented in Fig. 1. At low densities most molecules are in the vapor phase and the RDF obeys the analytical form of Eq. (40), above. At higher densities, and inside the phase transition region, the RDF shows an oscillatory behavior, which is typical of the liquidlike structure developed during condensation. At sufficiently large distances the intermolecular forces become negligible and the RDF approaches unity.

Given several simulation data, we represent the RDF  $g^{eq}(r; \rho)$  as a discrete function of density  $\rho$  and distance  $r$  and we determine  $a(\rho)$  directly from Eq. (16) using spline interpolations to determine accurately the integral in this equation. A typical result of such calculations is presented in Fig. 2 at a constant temperature,  $T^* = 1.25$ , showing that the first moment of force,  $a$ , is a strong function of density. Moreover,  $a$  is negative up to a certain density, above which it becomes positive. Since  $a$  is related to the compressibility factor of the fluid,  $z = P_0 / \rho k_B T$ , through Eq. (26), it is straightforward to conclude that at low densities  $z < 1$  because the attractive intermolecular forces cause the actual volume of the fluid to be less than its ideal value. At higher densities,  $z > 1$  tending to infinity at very high densities

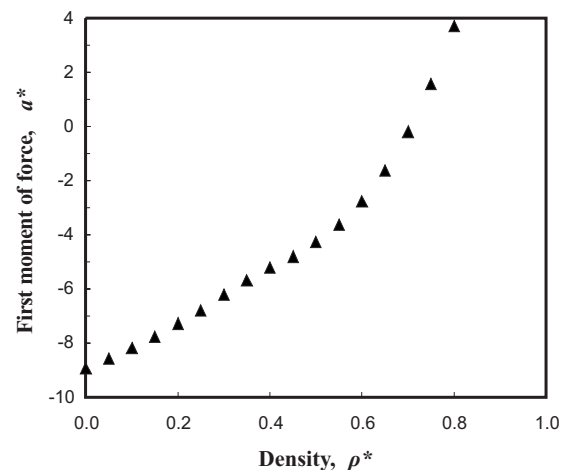
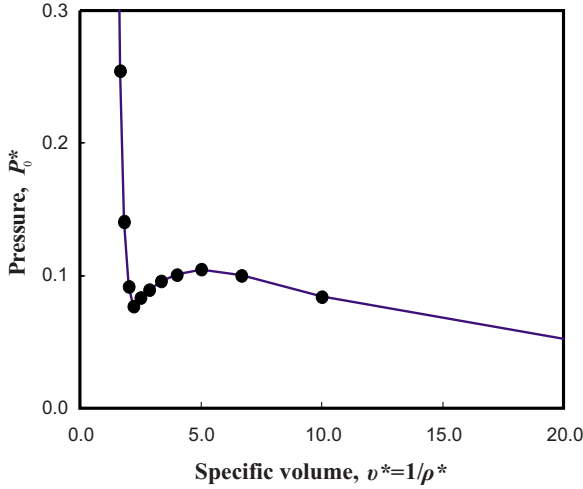


FIG. 2. Dependence of the first moment of force,  $a^*$ , on fluid density  $\rho^*$ , at  $T^* = 1.25$ .

FIG. 3. (Color online) Isotherm for a LJ fluid at  $T^*=1.25$ .

because the intermolecular repulsive forces cause the actual fluid volume to be greater than its ideal value.

Having determined  $a(\rho)$ , it is straightforward to compute the equation of state for a LJ fluid at a certain temperature [see Eq. (26)]. A typical isotherm is shown in Fig. 3. It is seen that this isotherm has qualitative similarities with the idealized Van der Waals equation of state.

The next step is to determine the saturation densities (gas and liquid) and saturation pressure, for a given temperature. This requires the simultaneous solution of the equations of pressure and chemical potentials that set the constraints for mechanical and chemical equilibrium, respectively (thermal equilibrium is already achieved since we work at constant temperature). An equivalent and simpler approach is to apply Maxwell's equal area rule, according to which

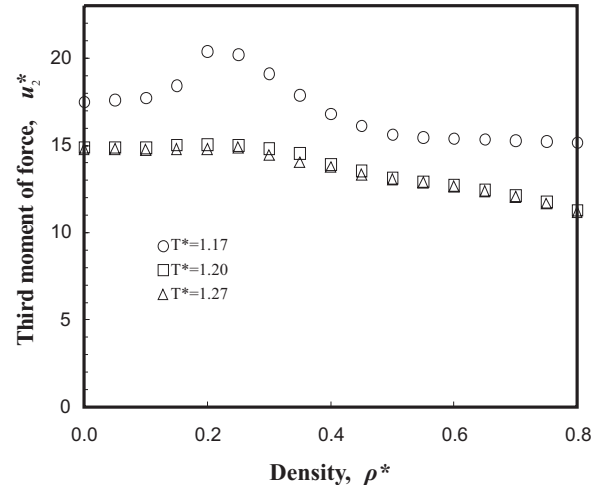
$$P_{0,s}(v_g - v_l) - \int_{v_l}^{v_g} P dv = 0, \quad (41)$$

where  $P_{0,s}$  is the saturation pressure, and,  $v_g$ ,  $v_l$  are the saturation specific volumes of gas and liquid at a certain temperature,  $T$ . Note that  $v=1/\rho$  assuming that  $v$  stands for the specific volume of the fluid.

The above procedure can be repeated at various temperatures in order to get the phase diagram for a LJ fluid. Note that in performing the above procedure we have assumed that Maxwell rule holds within the spinodal region of the isotherm [6], an assumption that is shown to be valid when the third moment of force,  $u_2$ , is constant [46].

## 2. Influence parameter

Extensive studies by McCoy *et al.* [8], have demonstrated that the third moment of force,  $u_2$ , is almost independent of density for fluids with various interaction potentials, including the classic 6–12 Lennard Jones potential. This result enables us to define the influence parameter,  $\kappa$ , as  $\kappa=u_2/2$ , which is also a density independent parameter [6,7]. In such a case it was shown before [7], that the gradient theory of the thermodynamic formulation, described by a third order differential equation, produces identical interfacial properties

FIG. 4. Dependence of the third moment of force,  $u_2$ , on fluid density,  $\rho^*$ , at different temperatures.

with the gradient theory of the mechanical formulation, which is described by a second order differential equation. This is a very important conclusion that enables us to utilize the BBGKY equations that describe, in general, momentum transfer under hydrostatic conditions in the more general case of equilibrium, where chemical equilibrium (equality of chemical potentials) must be imposed apart from mechanical equilibrium. To ensure that  $\kappa$  is indeed a weak function of density, we calculate the third moment of force,  $u_2$  from the integral in Eq. (17) at different densities and temperatures. The results are presented in Fig. 4. It is seen that  $u_2$  is almost density independent above  $T^*=1.2$  at least in the two-phase region. The behavior of  $u_2$  is different at  $T^*=1.17$  where we observe a distinct maximum in accord with similar studies [52,53]. Thus we expect that gradient theory and LBE model will be less accurate at temperatures below  $T^*=1.2$ .

From the above it is evident that the present LBE model, which originates from the BBGKY equations, should preserve mechanical and chemical equilibrium under the assumption that the influence factor,  $\kappa$ , does not depend on the fluid density  $\rho$ . This is shown to be true for the 6–12 LJ fluid, therefore the present LBE model appears to be thermodynamically consistent, as are the previously developed mean-field based models [23,35], having the additional advantage that thermodynamics is no longer described by semiempirical equations of state, but instead by the molecular interaction potential  $V(r)$ , a fundamental property that emanates from statistical mechanical theories.

Note that according to gradient theory the pressure tensor for the case of a constant influence parameter,  $\kappa$ , is given by [6,7,54]

$$\mathbf{P} = P_0 \mathbf{I} - \frac{\kappa}{3} \left\{ \left[ \rho \nabla^2 \rho - \frac{1}{2} (\nabla \rho)^2 \right] \mathbf{I} + 2 \left( \rho \nabla \nabla \rho - \frac{1}{2} \nabla \rho \nabla \rho \right) \right\}, \quad (42)$$

where  $P_0$  is the bulk fluid pressure given by Eqs. (26) or (27).

The only empirical parameter in the present LBE model is the mean collision time parameter,  $\lambda$ , which is related to the kinematic viscosity of the fluid through the standard equation (see for example [55]),

$$\nu = \frac{\eta}{\rho m} = \lambda \frac{k_B T}{m}. \quad (43)$$

Note that the above equation holds even for the case of a nonideal gas [56].

Unlike surface tension or other thermodynamic properties that can be described from straightforward (although complicated) integrals relating  $g^{eq}(r; \rho)$ ,  $V(r)$ , etc., transport properties including viscosity, thermal conductivity, and self-diffusion coefficient are much more difficult to be determined and only approximate expressions can be found from the kinetic theory of gases [57]. These expressions still require a series of calculations of complicated integrals making the whole approach of determining the above properties not very attractive.

Hence in the present study we choose a simpler and still quite accurate approach for the determination of viscosity from the LBE model as a function of density.

First we use equations from the literature that relate viscosity  $\eta$  as a function of density  $\rho$  for LJ fluids by fitting calculated viscosities from MD simulations to some semitheoretical expressions [58]. Then we solve Eq. (43) with respect to  $\lambda$  and get an expression for the latter parameter as function of density  $\rho$ . Finally we convert  $\lambda$  to  $\tau$ , which is the modified collision time employed in the discretized form of the LBE [11,12,35]. In essence, we follow the same procedure that was carried out before for the case of LBE models describing non-Newtonian fluids [59,60], where in the present case the expression for  $\lambda$  or  $\tau$  depends only on the fluid density,  $\rho$ , and not on velocity gradients as in the former case.

This approach guarantees that we will have the correct density dependence on viscosity for a LJ fluid. However, even if we had used a simple constant value for  $\tau$ , it would have no influence at all on the density profile, surface tension or any thermodynamic property (bulk or interfacial) of the fluid.

### B. Determination of bulk thermodynamic properties using the LBE model

The LBE model simulations have been performed using the two-dimensional (2D) nine-speed D2Q9 model for planar and circular interfaces. Technical details on the implementation of this model on Eqs. (33), (34), (35a), (35b), (36a), (36b), (37a)–(37c), (38), and (39) are given elsewhere [35,36]. For the case of planar interfaces we have used 100 pixels in the axial direction, where density variation takes place, with 30 pixels at each end occupied by low density values and the rest 40 pixels, located at the center, containing high density values. For the case of circular interfaces we have employed symmetric lattices of different size depending on the size of the circular drop or bubble, which varied from 40 up to 360 pixels, resulting in domains of  $100 \times 100$  up to  $460 \times 460$  pixels, respectively. In this case we

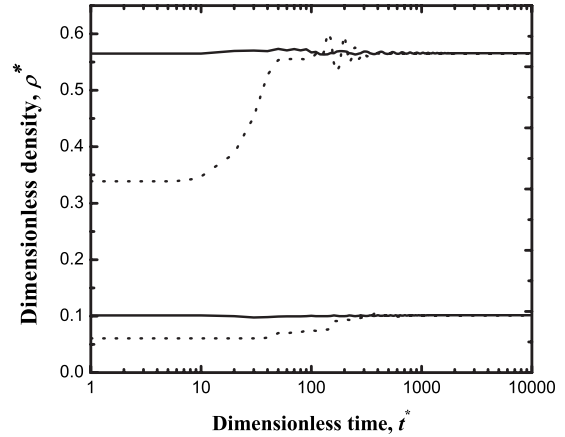


FIG. 5. Time evolution of bulk densities at  $T^* = 1.20$ . Solid line refers to initial densities equal to their vapor-liquid equilibrium values, while dotted line refers to initial densities that are 60% of their vapor-liquid equilibrium values.

place initially a circular or square region of high density at the center of the lattice the rest being occupied by low density values. Periodic boundary conditions are applied at each direction. To accelerate convergence to equilibrium we always assigned to the low and high densities the thermodynamic gas and liquid densities, respectively, computed from Maxwell's equal area rule at a specific temperature,  $T$ , although we have also performed studies starting from different initial densities to ensure uniqueness of the solution. For the case of planar interfaces it takes approximately 10 000–20 000 time steps to reach equilibrium, while for the case of a circular interface the number of time steps required increases by  $\sim 20$ – $30$  %. Note that equilibrium is established when fluid densities remain constant with time by an absolute error of  $< 10^{-6}$ , while at the same time the maximum parasitic velocity current is eliminated to round off [35]. Typical plots of density and velocity histories are presented in Figs. 5 and 6. It is observed that for a planar interface fluid densities can reach equilibrium after  $\sim 1000$ – $2000$  time steps and the rest of the time is needed for the parasitic velocity currents to drop down to values of the order of  $10^{-14}$ – $10^{-15}$ .

### Phase diagrams

In Tables I and II we compare the LBE model predictions of equilibrium densities, pressure and chemical potential with the exact solutions obtained from Maxwell's equal area rule. It is seen that the agreement is excellent for all bulk properties. Note that in all cases we used the lowest possible value of pixel size  $\delta x^*$  since we have seen from previous studies that the lower the pixel size (and hence the higher the resolution), the more accurate is the LBE model prediction [36]. Unfortunately we cannot use smaller values for  $\delta x^*$  due to stability issues that occur during the simulations (see also [36]).

Furthermore in Figs. 7 and 8, we compare the LBE predictions with those from molecular simulations for a LJ fluid [61–63]. Excellent agreement is found for all cases considered, indicating the validity of the present approach to de-

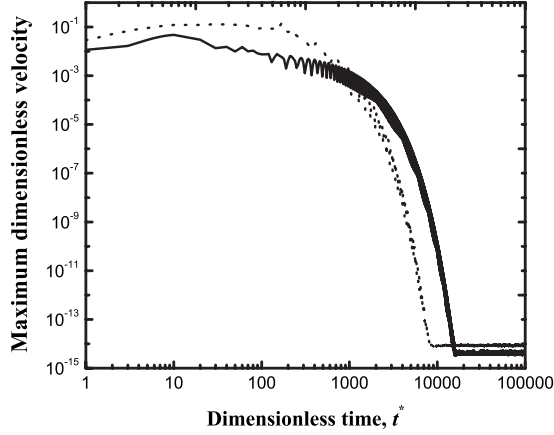


FIG. 6. Time evolution of maximum velocity at  $T^*=1.20$ . Solid line refers to initial densities equal to their vapor-liquid equilibrium values, while dotted line refers to initial densities that are 60% of their vapor-liquid equilibrium values.

scribe accurately the bulk thermodynamics of phase equilibrium for a LJ fluid. The present LBE model gives an excellent prediction of the bulk fluid properties for dimensionless temperatures  $T^*$  above 1.17. Below this temperature level, we have observed some stability issues in the simulations of the LBE model. Since for a LJ fluid the dimensionless critical temperature is  $T^* \sim 1.32$  we estimate a lower limit of the reduced temperature  $T_r = T/T_c$  of  $\sim 0.886$ , where we anticipate a breakdown of the gradient theory anyway.

The excellent agreement of the phase equilibrium properties predicted by the LBE model for a LJ fluid indicates that the current model preserves both chemical and mechanical equilibrium. Note that there have not been any literature results for the equilibrium chemical potential of a LJ fluid with the exception of the work by Lotfi *et al.* [61]. However, care must be taken in the definition of the chemical potential when comparing our present results with those in [61]. More specifically in [61], the results are given for the density-dependent part,  $\Delta\tilde{\mu}_0$ , of the chemical potential difference,  $\mu_0$ . Therefore, in order to compare our present results we must subtract the density independent properties  $k_B T(-\ln \rho_g + 1)$  from the right-hand side of Eq. (31). Through this approach we compute  $\Delta\tilde{\mu}_0^* = -2.94$  for  $T^* = 1.27$ , which is compared to  $\Delta\tilde{\mu}_0^* = -2.83$ , in [61]; and  $\Delta\tilde{\mu}_0^* = -3.27$  for  $T^* = 1.17$ , which is compared to  $\Delta\tilde{\mu}_0^* = -3.13$ , in [61]. It is seen that in both cases the relative error is less than 4.5%, in agreement

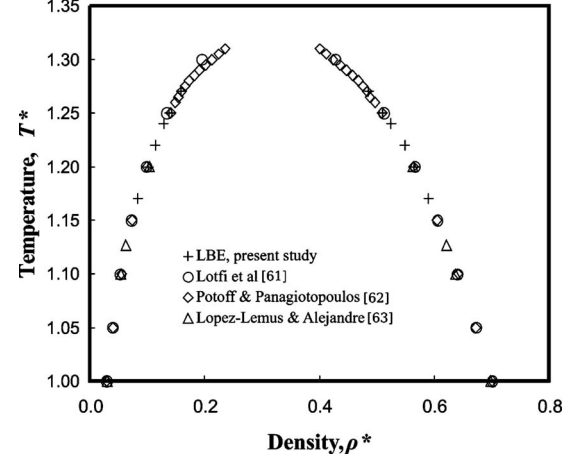


FIG. 7. Vapor and liquid coexisting densities as functions of temperature, for a LJ fluid.

with the error of pressure and equilibrium densities predicted from the present work compared to the respective properties in [61]. Thus we can conclude that our present work gives excellent predictions of all the basic bulk thermodynamic properties of a LJ fluid for  $T/T_c > 0.9$ .

### C. Determination of surface tension

#### 1. Planar interface

Following the gradient theory of the thermodynamic approach [3–6], the surface tension of a fluid for the case of a 1D planar interface (assuming that density  $\rho$  varies only along the  $x$  direction) is computed by the following formula:

$$\gamma = \int_{-\infty}^{\infty} \kappa \left( \frac{d\rho}{dx} \right)^2 dx. \quad (44)$$

On the other hand, following the mechanical definition of the surface tension through the pressure tensor [2,64], we have

$$\gamma = \int_{-\infty}^{\infty} \left( P_{xx} - \frac{(P_{yy} + P_{zz})}{2} \right) dx, \quad (45)$$

where  $P_{xx}$  is the normal component of the pressure tensor assumed to be uniform, while  $P_{yy} = P_{zz}$  are the tangential components that depend on distance,  $x$ . From Eq. (42) we get the following expressions for the components of the pressure tensor for a 1D planar interface:

TABLE I. Equilibrium densities for a LJ fluid.

$T^*$	Maxwell's rule		$\delta x^*$	LBE model	
	$\rho_g^*$	$\rho_l^*$		$\rho_g^*$	$\rho_l^*$
1.17	0.0835	0.5897	2.97	0.0839	0.5903
1.20	0.1013	0.5650	2.60	0.1018	0.5656
1.22	0.1140	0.5483	2.35	0.1144	0.5488
1.24	0.1286	0.5246	2.20	0.1286	0.5245
1.25	0.1384	0.5096	2.10	0.1384	0.5095
1.27	0.1591	0.4860	2.00	0.1591	0.4860

TABLE II. Equilibrium pressures and chemical potentials for a LJ fluid.

$T^*$	Maxwell's rule		$\delta x^*$	LBE model	
	$P_0^*$	$\Delta\mu_0^*$		$P_0^*$	$\Delta\mu_0^*$
1.17	0.0668	0.8004	2.97	0.0676	0.7987
1.20	0.0782	0.7721	2.60	0.0788	0.7714
1.22	0.0856	0.7510	2.35	0.0860	0.7495
1.24	0.0934	0.7261	2.20	0.0934	0.7262
1.25	0.0977	0.7057	2.10	0.0977	0.7057
1.27	0.1065	0.6694	2.00	0.1065	0.6694

$$P_{xx} = P_0 + \frac{\kappa}{2} \left( \frac{d\rho}{dx} \right)^2 - \kappa \rho \frac{d^2\rho}{dx^2}, \quad (46a)$$

$$P_{yy} = P_{zz} = P_0 + \frac{\kappa}{6} \left( \frac{d\rho}{dx} \right)^2 - \frac{\kappa}{3} \rho \frac{d^2\rho}{dx^2}. \quad (46b)$$

Comparing Eqs. (39) it is easy to show that

$$P_{yy} = P_{zz} = \frac{1}{3}P_{xx} + \frac{2}{3}P_0, \quad (47)$$

which is a well known result that relates the normal with the tangential components of the pressure tensor for a planar interface (e.g., [6,7] and references cited therein).

Substituting the above equations in Eq. (45) and integrating by parts with the additional boundary conditions that  $\frac{d\rho}{dx}=0$  at  $x \rightarrow \pm\infty$ , we can recover Eq. (44). Note that the equivalence of Eqs. (44) and (45) holds only when  $\kappa$  is density independent. If this is not the case, then the two expressions are no longer equivalent [7] and this causes a serious limitation of the current theory. Moreover, according to gradient theory, the density profile for a planar interface can be determined from the following integral equation:

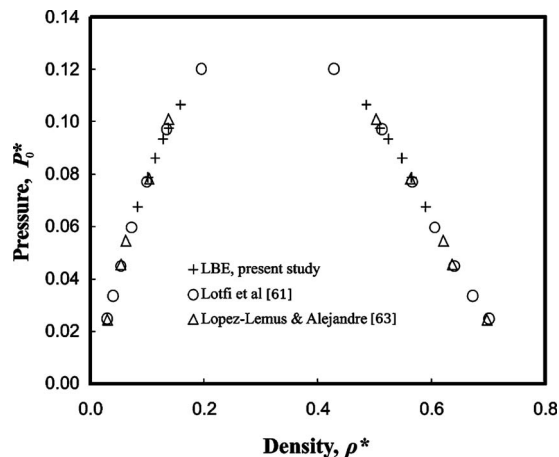


FIG. 8. Vapor and liquid coexisting densities as functions of pressure, for a LJ fluid.

$$x - x_a = \int_{\rho_a}^{\rho} \frac{d\rho'}{\varphi(\rho')}, \quad (48)$$

where  $\rho_a = \rho(x_a)$  [5,7]. In general, we choose  $x_a=0$  and then assign to  $\rho_a$  an arbitrary value between  $\rho_g$  and  $\rho_l$ . In the present study, we have chosen  $\rho_a = (\rho_g + \rho_l)/2$ , although more complicated choices, based on the Gibbs dividing surface of zero excess matter, have appeared in the literature [5].

Variable  $\varphi(\rho)$  in Eq. (48) is defined by

$$\varphi(\rho) = \frac{d\rho}{dx} \quad (49)$$

and  $\varphi(\rho)$  is determined from the following integral:

$$\varphi^2 = 2 \int_{\rho_l}^{\rho} \frac{\rho[P_0(\rho') - P_0(\rho_l)]}{\kappa\rho'^2} d\rho'. \quad (50)$$

Using Eq. (44) it is straightforward to show that [7]

$$\gamma = \int_{\rho_l}^{\rho_g} \kappa \cdot \varphi(\rho) d\rho. \quad (51)$$

The advantage of Eq. (51) over Eq. (45) is that in the former we do not need to calculate the density profile to determine the surface tension. This is very useful particularly when the density profiles get very steep as we move away from the critical temperature [5].

Our simulation results on surface tension are shown in Table III. It is seen that the surface tension predictions of the LBE model are in excellent agreement with the predictions from gradient theory. This is further illustrated in Fig. 9, where we compare the density profile obtained from the LBE simulation with that from the numerical solution of Eq. (48). These profiles are in excellent agreement indicating a close matching of the LBE model with gradient theory based on the mechanical approach.

Looking at the results in Table III, we note that when we compare surface tension values obtained from gradient theory with those from the LBE model, the predictions of the latter based on Eq. (44) are slightly worse than those from Eq. (45) for all temperatures. Furthermore, the difference between the two predictions becomes larger as the temperature decreases. To investigate this further we plot the integrands for each case in Fig. 10. In the same figure we compare them with the respective curves obtained from gradient

TABLE III. Surface tensions predicted by gradient theory for a planar interface.

$T^*$	Exact result		LBE model	
	$\gamma^*$ Eq. (44)	$\delta x^*$	$\gamma^*$ Eq. (37)	$\gamma^*$ Eq. (38)
1.17	0.1980	2.97	0.1790	0.2000
1.20	0.1409	2.60	0.1309	0.1410
1.22	0.1145	2.35	0.1085	0.1137
1.24	0.0810	2.20	0.0784	0.0806
1.25	0.0673	2.10	0.0655	0.0671
1.27	0.0440	2.00	0.0432	0.0439

theory. Note that in the latter we use Eq. (51) to compute surface tension, which is an integral in the density space, and hence does not involve accuracy limitations due to the profile steepness. Nevertheless, it is straightforward to obtain the detailed structure of the integrands of Eqs. (44) or (45) with the aid of Eqs. (48)–(51) for the case of gradient theory.

It is seen that due to the steepness of the density profile, the nonzero points in the integrand of Eq. (44) are not enough for very accurate integral calculations, compared to those in the integrand of Eq. (45). This problem deteriorates as the temperature decreases since we know that the interface thickness scales with a power law with temperature, and therefore the density profiles will get steeper as temperature decreases. An additional complication comes from the use of larger pixel sizes  $\delta x^*$  as temperature decreases for stability reasons (see also the analysis in [36]). Therefore the only possibility for an improvement in the accuracy of the surface tension computations is to introduce more points in the integrand of Eq. (44) using interpolation schemes. For example if we double the number of points in the density profile at  $T^*=1.25$ , using linear interpolation, we get from Eq. (44) a surface tension prediction of,  $\gamma^*=0.0670$ , which is in much closer comparison with the value predicted from gradient theory ( $\gamma^*=0.0673$ ). Further increase of the number of interpolating points by another factor of two, results in a surface tension prediction of  $\gamma^*=0.0673$ , which is in exact agree-

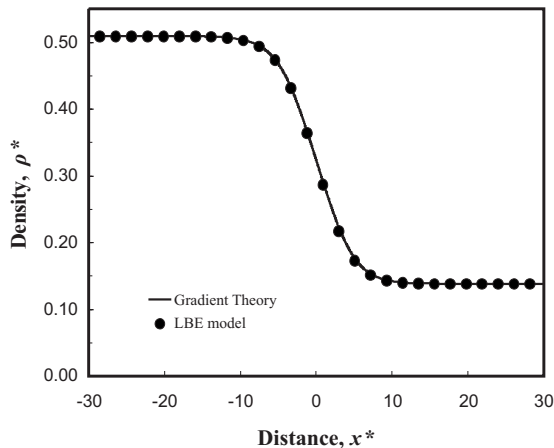


FIG. 9. Density profile for the case of a planar interface computed by the LBE model (filled points) and gradient theory (solid line).

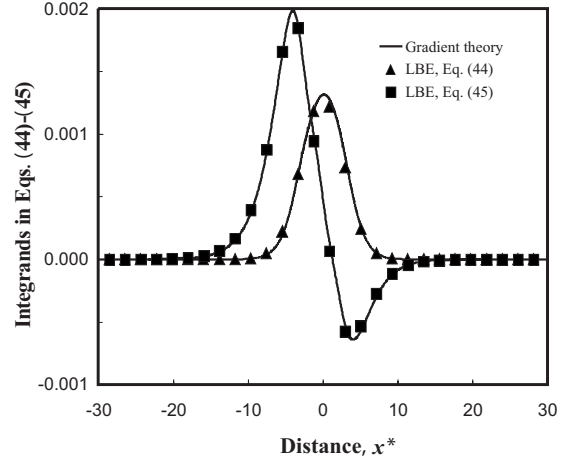


FIG. 10. Integrand profiles in Eqs. (44) and (45) for the case of a planar interface computed by the LBE model (filled points) and gradient theory (solid line).

ment with the value predicted from gradient theory as can be seen in Table III. The same behavior is observed qualitatively at all temperatures studied in this work. Note that if we use Eqs. (44) or (45) for the density results of gradient theory [instead of Eq. (51)] we will get the same value for  $\gamma^*$  that Eq. (51) predicts, provided that we use a sufficiently large number of points in space (typically of the order of 1000).

In Fig. 11 we compare the surface tension predictions of the present study with literature results from molecular simulation studies [63,65–67]. The observed discrepancies in the simulation results taken from the literature are attributed to the fact that different approaches have been used to simulate surface tension. These approaches are often different in nature (e.g., molecular dynamics are based on the mechanical definition of surface tension, while test area simulation or Monte Carlo methods are based on the thermodynamic definition of this property). Furthermore the use of a spherical cutoff in the molecule-molecule interactions has an important effect on surface tension predictions. Some authors have included long-range corrections (LRC) in surface tension predictions known as surface tail corrections which have re-

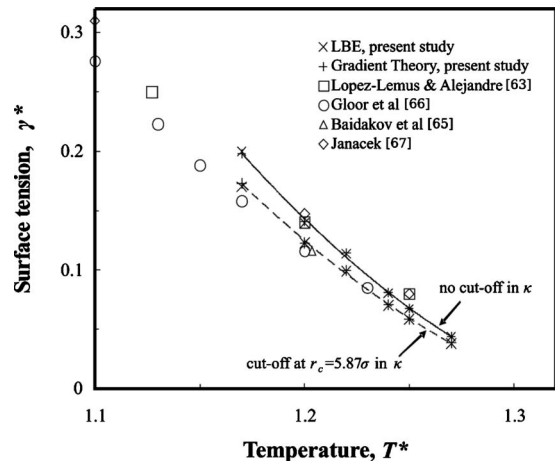


FIG. 11. Surface tension as a function of temperature, for a LJ fluid. Solid line is used to guide the eye through the LBE results.

sulted in an upward shift in the surface tension curve as a function of temperature. Our simulation results (both LBE model and gradient theory) appear to be closer to the LRC-corrected surface tensions. This is justified by the fact that we have not used any cutoff in the force term of the interaction potential appearing in the integral that defines the influence parameter,  $\kappa$ . Thus the spherical cutoff of  $5.87\sigma$  employed in the MD simulations to obtain  $g^{eq}(r; \rho)$  has a much smaller effect on the determination of the influence parameter compared to the interaction force  $\frac{\partial V}{\partial r}$  that is kept nonzero beyond the cutoff value. To further support our argument, we repeated our simulations applying the spherical cutoff in the interaction force and hence in the integral used to compute  $\kappa$ . The results are also presented in Fig. 11. It is seen that surface tension predictions are lower when spherical cutoff is applied in the determination of the influence factor  $\kappa$ . The surface tension predictions of the LBE model are again in close agreement with those of gradient theory and are in very good agreement with literature results where a similar spherical cutoff is employed with no surface tail corrections [65,66].

From the above results made on planar interfaces, it is evident that the LBE model predictions are in excellent agreement with gradient theory, on which the model is based. Any limitation of these predictions with respect to molecular simulation studies depends exclusively on the physical limitations of gradient theory and also on the approaches used to describe the radial distribution function  $g^{eq}(r; \rho)$ .

## 2. Curved interfaces

The case of a curved interface is more complicated to analyze because there are more nonvanishing terms in the pressure tensor given by Eq. (42). As a result we cannot use the simple Eqs. (44) or (45) as in the planar case. Instead, by applying the condition of mechanical equilibrium  $\nabla \cdot \mathbf{P} = 0$  we can obtain Laplace's law for a spherical or cylindrical liquid droplet [54],

$$\Delta P = P_{in} - P_{out} = \frac{s\gamma}{R_c}, \quad (52)$$

where  $\Delta P$  is the pressure difference between the center of the drop and the bulk of the surrounding gas phase, calculated from the respective density values through the respective equation of state,  $R_c$  is the drop radius,  $\gamma$  is the surface tension for the curved interface and  $s$  is a numerical shape factor due to the curvature effects. It is straightforward to show that for spherical drops  $s=2$ , while for circular drops  $s=1$ .

In Fig. 12 we present a plot of  $\Delta P$  vs  $1/R_c$  at  $T^*=1.25$  and  $T^*=1.27$ . It is seen that Laplace's law is verified at both temperatures. Furthermore, the value of surface tension obtained from the slope of  $\Delta P$  vs  $1/R_c$ , according to Eq. (52), is in very good agreement with the respective value computed for the case of planar interfaces.

A final remark is that in all simulations conducted with the present LBE model we have determined maximum values of parasitic current velocities of the order of  $10^{-14}$ – $10^{-15}$ , in accord with previous studies [35,36]. Hence the proposed model can simulate more realistic fluids using

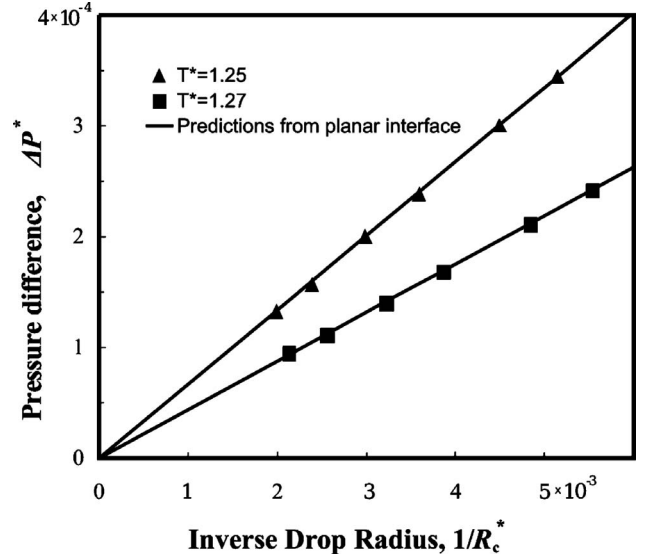


FIG. 12. Verification of Laplace's law for a LJ fluid using the LBE method.

input from statistical mechanics, while keeping the advantages of previously employed discretization schemes.

## IV. CONCLUSIONS

In the present work we have developed a lattice Boltzmann equation (LBE) model that originates from the discrete BBGKY evolution equations and is based on the mechanical approach of gradient theory of interfaces. The basic input of the model is the radial distribution function that is directly related to the molecular interaction potential and is provided from independent molecular simulations or from approximate theories.

We have applied the new model to obtain equilibrium bulk thermodynamic properties including phase equilibrium densities, pressure and chemical potential, for a Lennard-Jones (LJ) fluid at different temperatures. Excellent agreement is achieved between the LBE model and gradient theory as well as with independent literature results based on various molecular simulation approaches. Furthermore, surface tensions are computed at different temperatures for the case of planar and curved interfaces. Again excellent agreement is achieved between the proposed LBE model and gradient theory as well as with independent literature results obtained from molecular simulations. The results of this study indicate that the proposed LBE model can capture accurately bulk and interfacial thermodynamics for a LJ fluid at  $T/T_c > 0.9$ . Current focus of our work is to include surface-fluid interactions to study equilibrium and transport phenomena of real fluids on solid surfaces or within confined spaces.

## ACKNOWLEDGMENT

The work of A.G.Y. was supported by the EC FP7 under Grant Agreement No. 229773 (PERL). This funding is gratefully acknowledged.

- [1] R. Evans, *Adv. Phys.* **28**, 143 (1979).
- [2] J. S. Rowlinson and B. Widom, *Molecular Theory of Capillarity* (Clarendon Press, New York, 1989).
- [3] J. W. Cahn and J. E. Hilliard, *J. Chem. Phys.* **28**, 258 (1958).
- [4] A. J. M. Yang, P. D. Fleming III, and J. H. Gibbs, *J. Chem. Phys.* **64**, 3732 (1976).
- [5] V. Bongiorno and H. T. Davis, *Phys. Rev. A* **12**, 2213 (1975).
- [6] H. T. Davis and L. E. Scriven, *Adv. Chem. Phys.* **49**, 357 (1982).
- [7] B. S. Carey, L. E. Scriven, and H. T. Davis, *J. Chem. Phys.* **69**, 5040 (1978).
- [8] B. F. McCoy, L. E. Scriven, and H. T. Davis, *J. Chem. Phys.* **75**, 4719 (1981).
- [9] J. A. Barker and D. Henderson, *Rev. Mod. Phys.* **48**, 587 (1976).
- [10] J.-P. Hansen and I. R. McDonald, *Theory of Simple Liquids* (Elsevier Academic Press, London, 1990).
- [11] R. Benzi, S. Succi, and M. Vergassola, *Phys. Rep.* **222**, 145 (1992).
- [12] S. Chen and G. Doolen, *Annu. Rev. Fluid Mech.* **30**, 329 (1998).
- [13] C. K. Aidun and J. R. Clausen, *Annu. Rev. Fluid Mech.* **42**, 439 (2010).
- [14] S. Succi, I. V. Karlin, and H. Chen, *Rev. Mod. Phys.* **74**, 1203 (2002).
- [15] X. Shan and H. Chen, *Phys. Rev. E* **47**, 1815 (1993).
- [16] X. Shan and H. Chen, *Phys. Rev. E* **49**, 2941 (1994).
- [17] N. S. Martys and H. Chen, *Phys. Rev. E* **53**, 743 (1996).
- [18] J. Zhang, B. Li, and D. Y. Kwok, *Phys. Rev. E* **69**, 032602 (2004).
- [19] R. Benzi, L. Biferale, M. Sbragaglia, S. Succi, and F. Toschi, *Phys. Rev. E* **74**, 021509 (2006).
- [20] M. Sbragaglia, R. Benzi, L. Biferale, S. Succi, K. Sugiyama, and F. Toschi, *Phys. Rev. E* **75**, 026702 (2007).
- [21] X. He and L.-S. Luo, *Phys. Rev. E* **56**, 6811 (1997).
- [22] S. Ansumali and I. V. Karlin, *Phys. Rev. Lett.* **95**, 260605 (2005).
- [23] X. He and G. D. Doolen, *J. Stat. Phys.* **107**, 309 (2002).
- [24] N. S. Martys, *Physica A* **362**, 57 (2006).
- [25] A. Xu, S. Succi, and B. M. Boghosian, *Math. Comput. Simul.* **72**, 249 (2006).
- [26] X. He, X. Shan, and G. D. Doolen, *Phys. Rev. E* **57**, R13 (1998).
- [27] L.-S. Luo, *Phys. Rev. Lett.* **81**, 1618 (1998).
- [28] L.-S. Luo, *Phys. Rev. E* **62**, 4982 (2000).
- [29] Y. Shi, T. S. Zhao, and Z. L. Guo, *Phys. Rev. E* **73**, 026704 (2006).
- [30] P. L. Bhatnagar, E. Gross, and M. Krook, *Phys. Rev.* **94**, 511 (1954).
- [31] X. He, S. Chen, and R. Zhang, *J. Comput. Phys.* **152**, 642 (1999).
- [32] A. Cristea, G. Gonnella, A. Lamura, and V. Sofonea, *Math. Comput. Simul.* **72**, 113 (2006).
- [33] A. J. Wagner, *Phys. Rev. E* **74**, 056703 (2006).
- [34] T. Lee and C.-L. Lin, *J. Comput. Phys.* **206**, 16 (2005).
- [35] T. Lee and P. F. Fischer, *Phys. Rev. E* **74**, 046709 (2006).
- [36] E. S. Kikkinides, A. G. Yiotis, M. E. Kainourgiakis, and A. K. Stubos, *Phys. Rev. E* **78**, 036702 (2008).
- [37] D. Chiappini, G. Bella, S. Succi, F. Toschi, and S. Ubertini, *Comm. Comp. Phys.* **7**, 423 (2010).
- [38] P. Yuan and L. Schaefer, *Phys. Fluids* **18**, 042101 (2006).
- [39] R. S. Qin, *Phys. Rev. E* **73**, 066703 (2006).
- [40] S. Chibbaro, G. Falcucci, G. Chiatti, H. Chen, X. Shan, and S. Succi, *Phys. Rev. E* **77**, 036705 (2008).
- [41] S. Melchionna and U. Marini Bettolo Marconi, *EPL* **81**, 34001 (2008).
- [42] K. Huang, *Statistical Mechanics* (Wiley, New York, 1987).
- [43] J. Frey, J. Salmon, and M. Valton, *J. Stat. Phys.* **11**, 457 (1974).
- [44] T. Ihle and D. M. Kroll, *Comput. Phys. Commun.* **129**, 1 (2000).
- [45] H. T. Davis and L. E. Scriven, *J. Chem. Phys.* **69**, 5215 (1978).
- [46] E. C. Aifantis and J. B. Serrin, *J. Colloid Interface Sci.* **96**, 517 (1983).
- [47] Y. Tang and B. C.-Y. Lu, *AIChE J.* **43**, 2215 (1997).
- [48] M. P. Allen and D. J. Tildesley, *Computer Simulation of Liquids* (Oxford University Press, Oxford, 1987).
- [49] A. Trokhymchuk and J. Alejandre, *J. Chem. Phys.* **111**, 8510 (1999).
- [50] D. O. Dunikov, S. P. Malysenko, and V. V. Zhakhovskii, *J. Chem. Phys.* **115**, 6623 (2001).
- [51] K. Refson, <http://www.ccp5.ac.uk/moldy/moldy.html>
- [52] P. M. W. Cornelisse, C. J. Peters, and J. de Swaan Arons, *J. Chem. Phys.* **106**, 9820 (1997).
- [53] V. G. Baidakov, S. P. Protsenko, G. G. Chernykh, and G. Sh. Boltachev, *Phys. Rev. E* **65**, 041601 (2002).
- [54] A. H. Falls, L. E. Scriven, and H. T. Davis, *J. Chem. Phys.* **75**, 3986 (1981).
- [55] S. Succi, *The Lattice-Boltzmann Equation: For Fluid Dynamics and Beyond* (Clarendon Press, Oxford, 2001).
- [56] N. S. Martys, *Int. J. Mod. Phys. C* **10**, 1367 (1999).
- [57] G. H. A. Cole, *Rep. Prog. Phys.* **33**, 737 (1970).
- [58] R. L. Rowley and M. M. Painter, *Int. J. Thermophys.* **18**, 1109 (1997).
- [59] N. Rakotomalala, D. Salin, and P. Watzky, *Phys. Fluids* **8**, 3200 (1996).
- [60] J. Psihogios, M. E. Kainourgiakis, A. G. Yiotis, A. Papaioannou, and A. K. Stubos, *Transp. Porous Media* **70**, 279 (2007).
- [61] A. Lotfi, J. Vrabec, and J. Fischer, *Mol. Phys.* **76**, 1319 (1992).
- [62] J. J. Potoff and A. Z. Panagiotopoulos, *J. Chem. Phys.* **112**, 6411 (2000).
- [63] J. Lopez-Lemus and J. Alejandre, *Mol. Phys.* **100**, 2983 (2002).
- [64] J. G. Kirkwood and F. P. Buff, *J. Chem. Phys.* **17**, 338 (1949).
- [65] V. G. Baidakov, S. P. Protsenko, Z. R. Kozlova, and G. G. Chernykh, *J. Chem. Phys.* **126**, 214505 (2007).
- [66] G. J. Gloor, G. Jackson, F. J. Blas, and E. de Miguel, *J. Chem. Phys.* **123**, 134703 (2005).
- [67] J. Janeček, *J. Chem. Phys.* **131**, 124513 (2009).